Supplement of Nat. Hazards Earth Syst. Sci., 22, 1683–1698, 2022
https://doi.org/10.5194/nhess-22-1683-2022-supplement

Natural Hazards and Earth System Sciences
Open Access

Supplement of

The role of heat wave events in the occurrence and persistence of thermal stratification in the southern North Sea

Wei Chen et al.

Correspondence to: Wei Chen (wei.chen@hereon.de)

1 Results of uncoupled NEMO model run

Figure S1 is similar to Figure 3 of the main text but shows the model run where NEMO was uncoupled with WAM. Compared to the coupled model run, the water was colder near the bottom in the uncoupled run. For the sites with deeper depth, e.g., in the Dogger Bank and at NSB III, the water temperature of the uncoupled model run was closer to the observations. However, these results do not indicate a better performance of the uncoupled model in predicting temperature profiles of the North Sea. Further analysis of the multiple-year water temperatures of the uncoupled model run revealed that without considering the wave effect, the simulations generally underestimated the near-bottom temperatures by $2 \sim 3°$C during the warm period. Subsequently, the uncoupled model predicted a stronger thermal stratification. As shown in Figure S1, the uncoupled model failed to represent the temperature profiles at FINO-1. It yielded a larger vertical variance in water temperatures.

We further compared the coupled and the uncoupled runs within the area between the south of 50 m isobath and 3-8°E. Data in the Dogger Bank and at NSB III were used. The interannual variation in the seawater temperatures of the uncoupled run at the two stations was similar to that of the coupled run, except that the near-bottom temperature in the uncoupled run was colder than the data obtained from the coupled model run. Figure S2 is similar to Figure 2 of the main text but shows the uncoupled run. Note that the air temperature, prescribed as the forcing, was the same for both coupled and uncoupled runs and was thus not shown in Figure S2. In most years (except for 2018), the water temperature of the uncoupled model run was underestimated at the bottom. The difference between the MARNET data and the model reached $2 \sim 3°$C.

Figure S3 illustrates the spatial distribution of ϕ in each month of 2018 for the uncoupled model run. The annual cycle of ϕ is similar to Figure 7 of the main text. The southern North Sea was stratified from mid-spring and reached the maximum between late July and August. A division appeared around the 50 m isobath. Since September, the water column was well mixed in the south, whereas in the north, the water column remained stratified until November. The ϕ of the uncoupled run was greater than that of the coupled model run in the entire southern North Sea from March to November. During the summer period (from Jun to August), the maximum ϕ exceeded 1100 J m^{-3}, which was approximately 40% higher than that obtained in the coupled model run. Differences between the two runs were hardly observed in the winter period since the water column was well mixed.

Figure S4 is similar to Figure 8 of the main text but for the uncoupled run. Like the coupled model run, ϕ presents interannual variations in the southern North Sea. The stratification was weaker than the multiyear mean in 2011, 2012, 2015 and 2017 (mainly in the eastern part), whereas it was greater than the multiyear mean in 2013,2014 and 2018. Furthermore, ϕ of the uncoupled model run has larger interannual variations in the south of the 50 m isobaths, especially between 3-8°E. For example, in 2011 and 2017, the difference in ϕ was -200 J m^{-3} while it was -150 J m^{-3} in the coupled model run. In the coupled model run, the maximum interannual variation occurred near the northern boundary of the southern North Sea.

Figure S5 shows the correlation of the air temperatures to the thermal stratification (quantified with ϕ) computed from the uncoupled model water temperatures. The correlation coefficient $R > 0.5$ covered the region of seasonal stratification, which was consistent with that of the coupled model run. In the Norwegian Trench and the Dutch Coast, where stratification was not caused by the thermocline, R illustrated a spatial pattern similar to that of the coupled model run. However, in the uncoupled run, the area of the permanent mixed region was smaller. Close to the Wadden Sea, $0 < R < 0.4$. Meanwhile, negative R was obtained in a larger area in the German Bight.

Figure S6 is similar to Figure 10 of the main text, but for the uncoupled model run. Although the overall spatial pattern of r was similar to that of the coupled model run, its value is smaller. In the seasonally stratified region ($R > 0.6$), r was approximately 0. In other words, the number of days when the water is stratified during the warm season (May to August) remained the same each year. In the uncoupled model run, the seasonal stratification was partly dominant in the south of the 50 m isobaths, especially around the Dogger Bank. The region where large r appeared was mostly near the southern coast of the North Sea, with the maximum value located west of the Danish Wadden Sea.

Like Figure 11 in the main text, Figure S7 illustrates the ratio between the change in stratification days and the change in intensive air temperature incline. The maximum ratio was observed outside the Rhine estuary along the Belgium coast and close to the permanently mixed region. The stratification in this region is generated by the freshwater input from the Rhine River. The stratification becomes stronger and more stable due to the absence of turbulent mixing by the waves.

The gradient Richardson number R_i of the uncoupled model run (Figure S8) is compared with that of the coupled model run (see Figure 12 in the main text). For both 2015 and 2018, $\log_{10} R_i$ was larger and lasted longer than that in the coupled run.

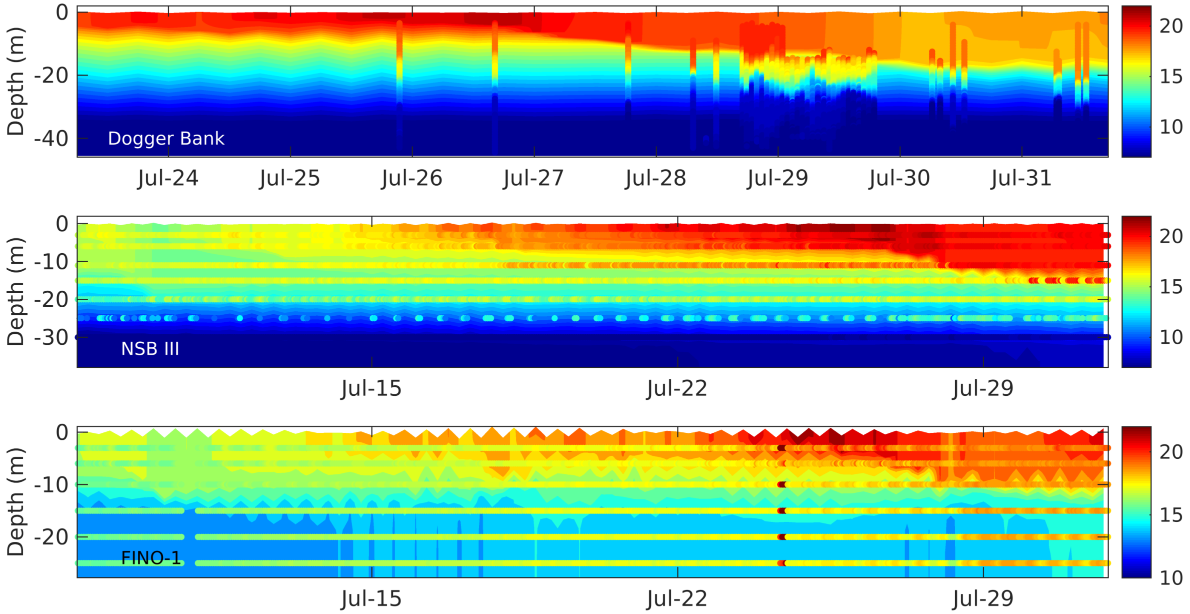

Figure S1. In situ-measured and uncoupled model-simulated water temperatures (in °C) in July. In the Dogger Bank, measurements were obtained by a CTD profiler during the Poseidon campaign. At the MARNET stations NSB III and FINO-1, temperatures were measured in fixed water layers.

At the Northsea Mid site, stable stratification lasted even until the end of the year. However, like the coupled run, $\log_{10} R_i > 1$ mainly occurred within 45 m. In the Dogger Bank and at NSB III, $\log_{10} R_i > 1$ was observed from the beginning of June until October in both 2015 and 2018. The R_i was much larger than the value obtained in the coupled model run. Moreover, large R_i (i.e., $\log_{10} R_i > 1$) reached 10 m above the bottom. At NSB III, small R_i in 2015 implied a homogeneous water column in the whole year. In 2018, large R_i appeared from mid-May to June 25 m above the bottom and from July until early September 20 m above the bottom. In this year, stratification developed in July and August in Fino-1.

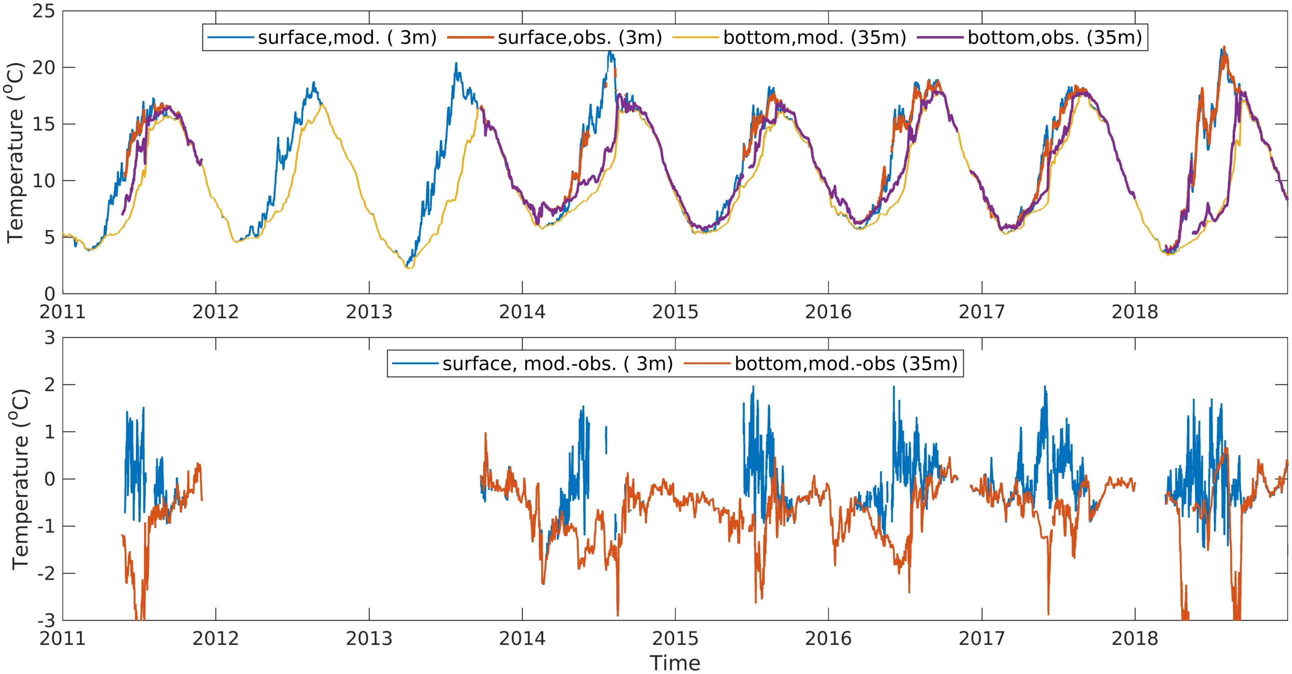

Figure S2. Upper panel: The interannual variation in the observed (obs.) and the uncoupled model simulated (mod.) water temperatures at the surface and the bottom of the same location. Lower panel: Water temperature differences between the model and the in situ measurements at the surface and the bottom.

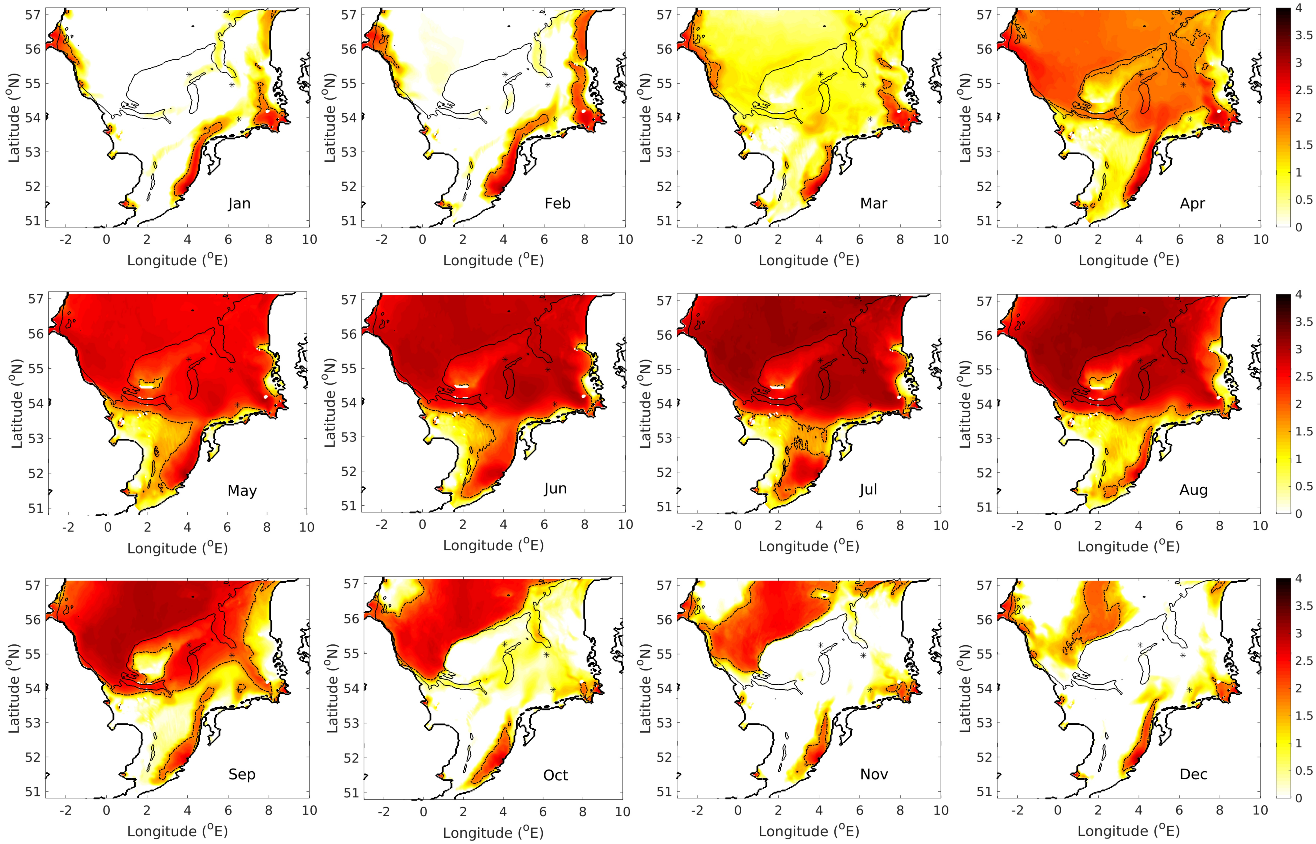

Figure S3. Evolution of the monthly mean potential energy anomaly ϕ (J m^{-3} on a $\log_{10}$ scale) for 2018. The dashed line indicates the location where $\phi = 50$ J m^{-3}. The water column is considered to be stratified when ϕ is above this value. Thin black lines indicate the location of the 50 m isobath.

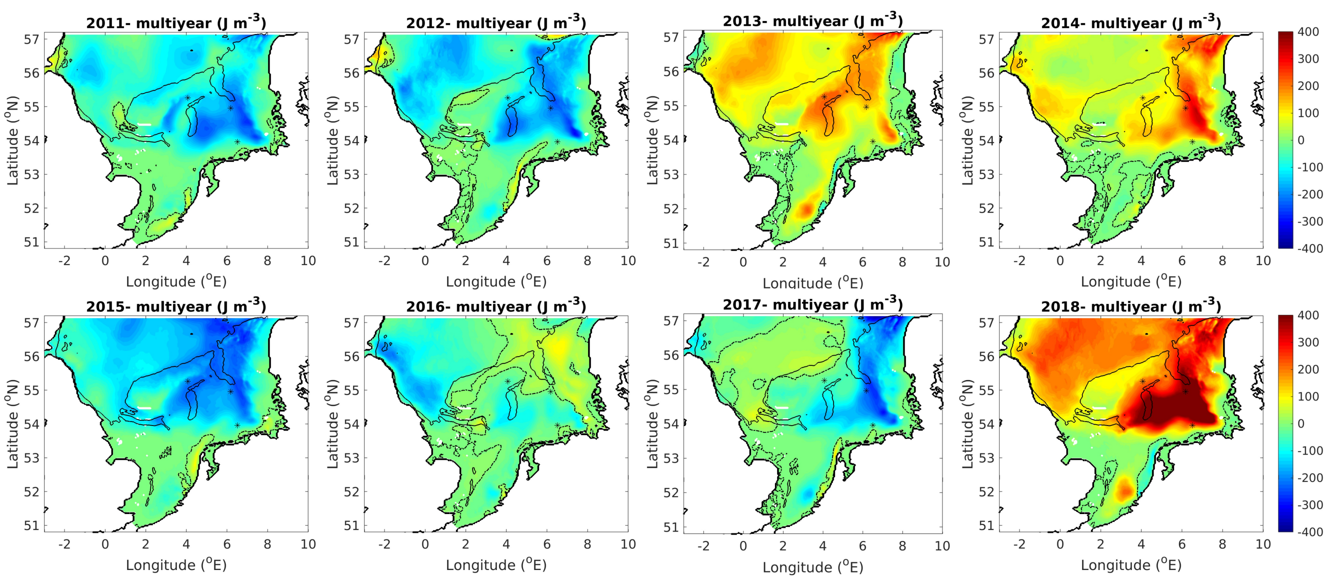

Figure S4. Difference in potential energy anomaly (J m^{-3}) averaged over three month (June, July and August) between a specific year and the multiyear mean. The dashed line indicates $\phi = 50$ J m^{-3}. Thin black lines indicate the location of the 50 m isobath.

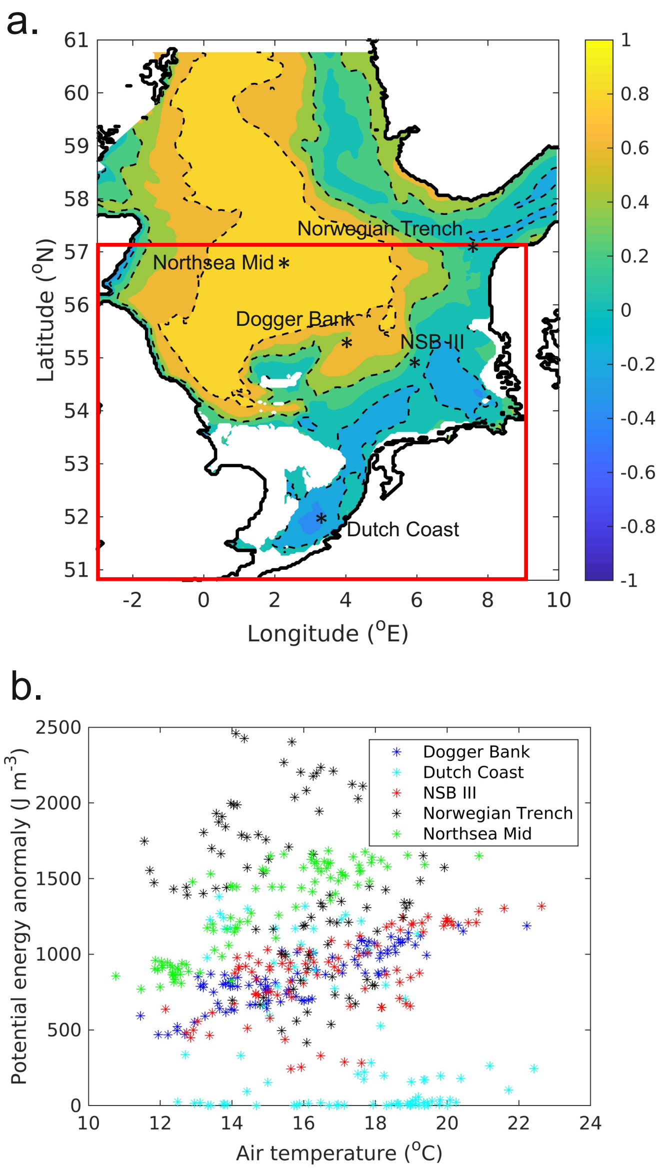

Figure S5. (a): Computed correlation coefficient R between the air temperature and the potential energy anomaly for summer 2018 (June, July and August). Note that the area with no stratification ($\phi < 50$ J m^{-3}) is excluded. Dashed contours indicate $R = 0, 0.4$ and 0.8. (b): Relationship between the air temperature and the potential energy anomaly in the different regimes of the North Sea. The locations are illustrated in (a). The red frame indicates the region of the southern North Sea.

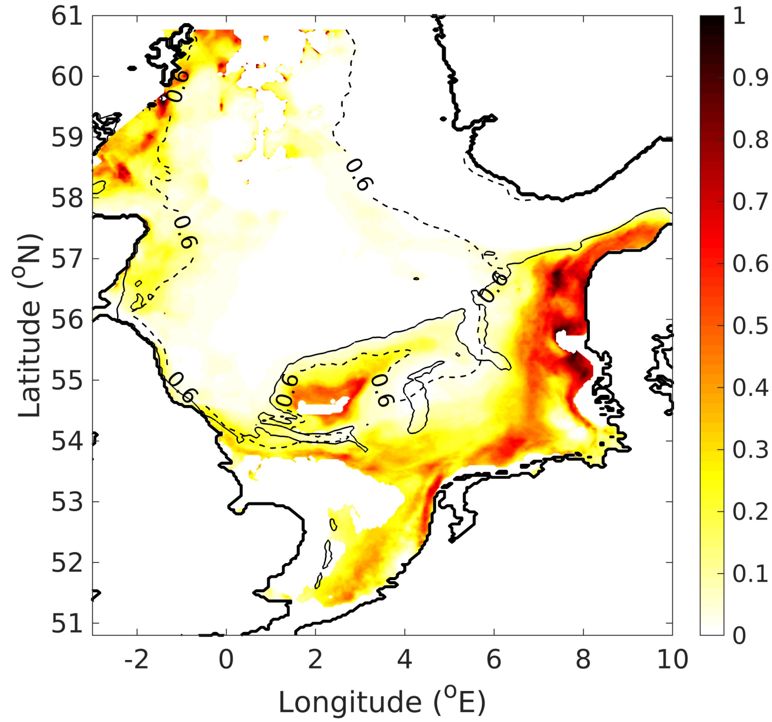

Figure S6. Ratio of the number of water stratification days to the number of MHW days. The dashed contour line corresponds to the correlation coefficient $R = 0.6$ between the air temperature and the potential energy anomaly for the multiyear mean of the summer time. The thin solid line indicates the 50 m isobath.

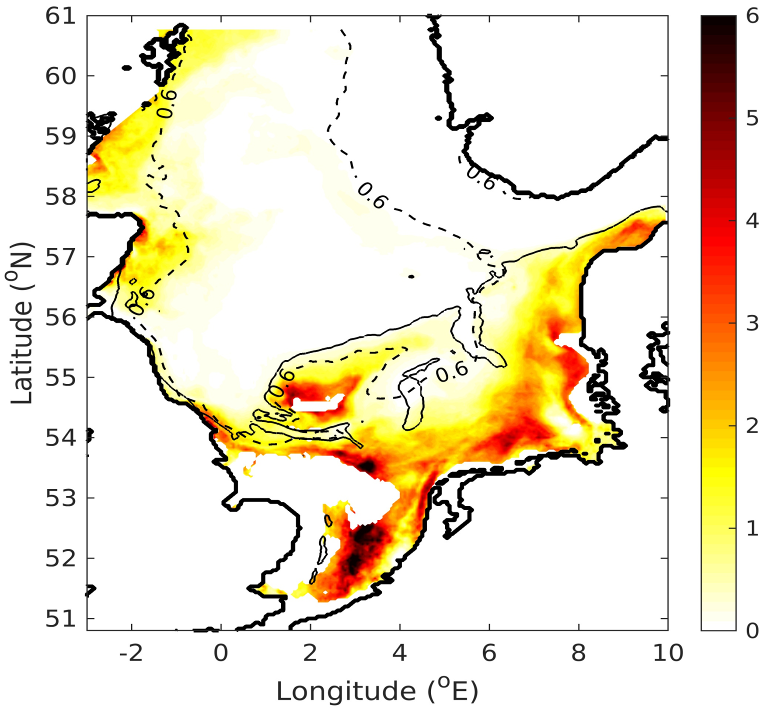

Figure S7. Ratio between the number of days when the water is stratified and the number of days when the air temperature intensively increases. The contour line with a value of 0.6 indicates the area with a correlation coefficient $R = 0.6$ between the air temperature and the potential energy anomaly for the multiyear mean of the summertime. The thin solid line indicates the 50 m isobath.

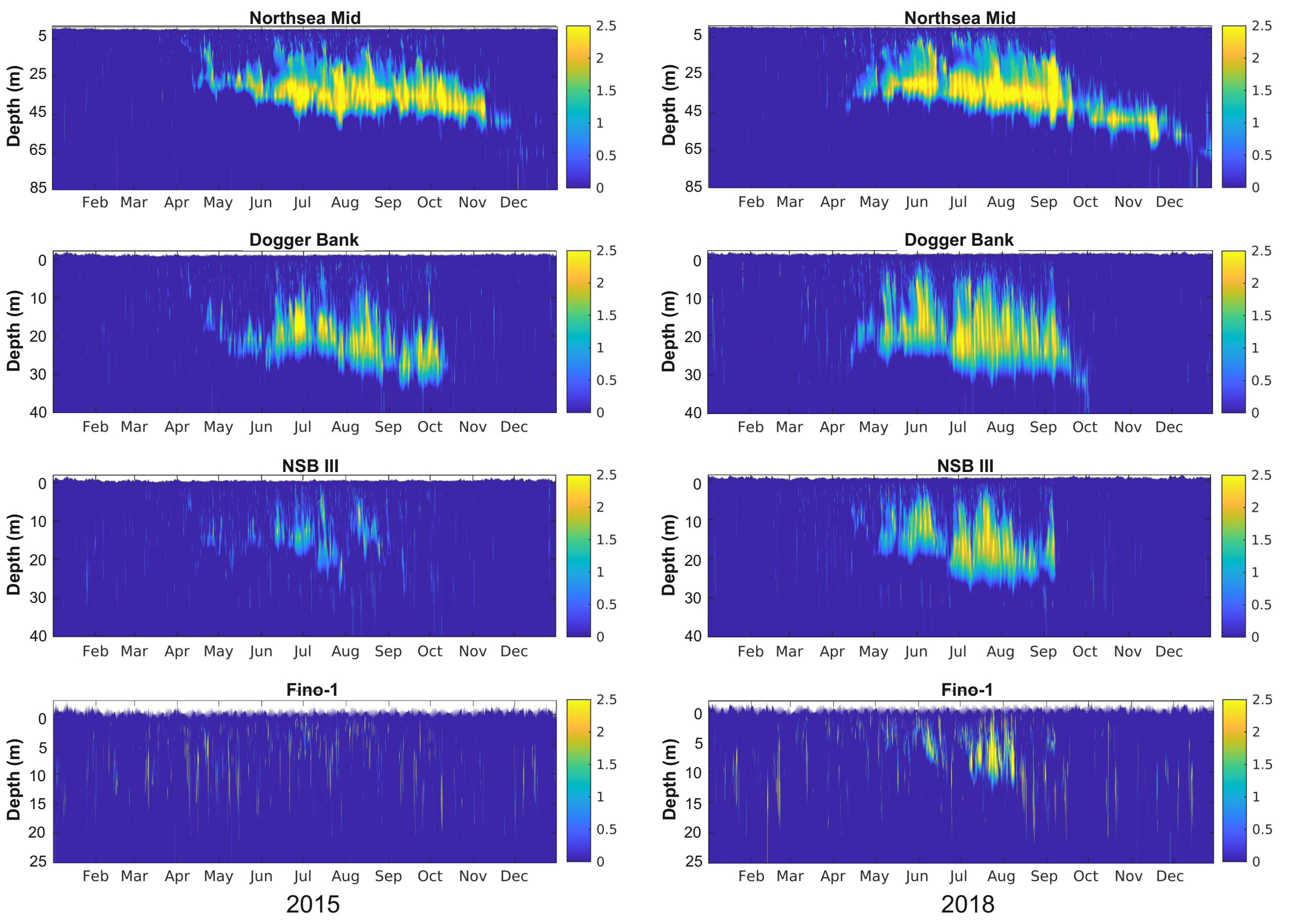

Figure S8. Gradient Ri for 2015 (left column) and 2018 (right column) at the Northsea Mid, Dogger Bank, NSB III and Fino-1 on a $\log_{10}$ scale.